Titre: Title:	Advanced 1D heterostructures based on nanotube templates and molecules. Supplément
Auteurs: Authors:	Charlotte Allard, Laurent Alvarez, Jean-Louis Bantignies, Nedjma Bendiab, Sofie Cambré, Stéphane Campidelli, Jeffrey Fagan, Emmanuel Flahaut, Benjamin S. Flavel, F. Fossard, Étienne Gaufrès, Sebastian Heeg, Jean-Sébastien Lauret, Annick Loiseau, Jean-Baptiste Marceau, Richard Martel, Laëtitia Marty, Thomas Pichler, Christophe Voisin, Stéphanie Reich, Antonio Setaro, Lei Shi, & Wim Wenseleers
Date:	2024
Type:	Article de revue / Article
Référence: Citation:	Allard, C., Alvarez, L., Bantignies, J.-L., Bendiab, N., Cambré, S., Campidelli, S., Fagan, J., Flahaut, E., Flavel, B. S., Fossard, F., Gaufrès, É., Heeg, S., Lauret, J.-S., Loiseau, A., Marceau, J.-B., Martel, R., Marty, L., Pichler, T., Voisin, C., ... Wenseleers, W. (2024). Advanced 1D heterostructures based on nanotube templates and molecules. Chemical Society Reviews, 56 pages. https://doi.org/10.1039/d3cs00467h

Titre de la revue: Journal Title:	Chemical Society Reviews
Maison d'édition: Publisher:	Royal Society of Chemistry
URL officiel: Official URL:	https://doi.org/10.1039/d3cs00467h
Mention légale: Legal notice:	This article is licensed under a Creative Commons Attribution-NonCommercial 3.0 Unported Licence.

Titre: Title:	Advanced 1D heterostructures based on nanotube templates and molecules. Supplément
Auteurs: Authors:	Charlotte Allard, Laurent Alvarez, Jean-Louis Bantignies, Nedjma Bendiab, Sofie Cambré, Stéphane Campidelli, Jeffrey Fagan, Emmanuel Flahaut, Benjamin S. Flavel, F. Fossard, Étienne Gaufrès, Sebastian Heeg, Jean-Sébastien Lauret, Annick Loiseau, Jean-Baptiste Marceau, Richard Martel, Laëtitia Marty, Thomas Pichler, Christophe Voisin, Stéphanie Reich, Antonio Setaro, Lei Shi, & Wim Wenseleers
Date:	2024
Type:	Article de revue / Article
Référence: Citation:	Allard, C., Alvarez, L., Bantignies, J.-L., Bendiab, N., Cambré, S., Campidelli, S., Fagan, J., Flahaut, E., Flavel, B. S., Fossard, F., Gaufrès, É., Heeg, S., Lauret, J.-S., Loiseau, A., Marceau, J.-B., Martel, R., Marty, L., Pichler, T., Voisin, C., ... Wenseleers, W. (2024). Advanced 1D heterostructures based on nanotube templates and molecules. Chemical Society Reviews, 56 pages. https://doi.org/10.1039/d3cs00467h

Titre de la revue: Journal Title:	Chemical Society Reviews
Maison d'édition: Publisher:	Royal Society of Chemistry
URL officiel: Official URL:	https://doi.org/10.1039/d3cs00467h
Mention légale: Legal notice:	This article is licensed under a Creative Commons Attribution-NonCommercial 3.0 Unported Licence.

Supporting Information of

Advanced 1D Heterostructures based on Nanotube Templates and Molecules

Authors, by alphabetical order: Charlotte Allard[1], Laurent Alvarez[2], Jean-Louis Bantignies[2], Nedjma Bendiab[3], Sofie Cambré[4], Stephane Campidelli[5] Jeffrey A. Fagan[6], Emmanuel Flahaut[7], Benjamin Flavel[8], Frederic Fossard[9], Etienne Gaufrès[10*], Sebastian Heeg[11], Jean-Sebastien Lauret[12], Annick Loiseau[9], Jean-Baptiste. Marceau[10], Richard Martel[13], Laetitia Marty[3] Thomas Pichler[14], Christophe Voisin[15], Stephanie Reich[16], Antonio Setaro[16,17], Lei Shi[17], Wim Wenseleers[4]

* Corresponding author: etienne.gaufres@cnrs.fr

1- Ecole Polytechnique, Montreal, Canada
2- CNRS-Université de Montpellier, France
3- CNRS-Université de Grenoble, France
4- University of Antwerp, Belgium
5- CEA-Saclay, France
6- National Institute of Standards and Technology (NIST), US
7- CIRIMAT, Université Toulouse 3 Paul Sabatier, Toulouse INP, CNRS, Université de Toulouse, 118 Route de Narbonne, 31062 Toulouse cedex 9 - France
8- Karlsruhe Institute of Technology (KIT), Germany
9- Laboratoire d'Étude des Microstructures, CNRS-Onera, Chatillon, France
10- Laboratoire Photonique, Numérique et Nanosciences, CNRS-Université de Bordeaux-IOGS, Talence, France
11- Humboldt-Universität zu Berlin, Germany
12- LUMIN, Université Paris Saclay, ENS Paris Saclay, CentraleSupelec, CNRS, Orsay, France
13- University of Montreal, Canada
14- University of Vienna, Austria
15- Université de Paris, Ecole Normale Paris, CNRS, PSL, France
16- Free University of Berlin, Germany
17- Faculty of Engineering and Informatics, Pegaso University, Naples, Italy.
18- State Key Laboratory of Optoelectronic Materials and Technologies, Guangdong Basic Research Center of Excellence for Functional Molecular Engineering, Nanotechnology and Research Center, School of Materials Science and Engineering, Sun Yat-sen University, Guangzhou, 510275, China

Table of contents.

S1 Different methods to prepare NT based heterostructures.

S1.1 Opening of CNTs and BNNTs

After synthesis, single-walled carbon nanotubes (SWCNTs) are typically closed at both ends. Aside from SWCNTs, synthesized SWCNT powders also contain amorphous carbon, graphitic carbon shells (around the catalytic particles) and other carbonaceous materials.[1] A typical opening procedure comprises 3 steps: a first oxidation step, followed by a treatment in strong acids and a final annealing step to remove all encapsulated solvents or external functional groups that are introduced during the opening procedure. Since such an opening procedure is very similar to the typically applied purification protocols for SWCNTs,[2,3] most purified SWCNT samples are already unintentionally opened, and need no further treatment (except for the final annealing step).

In fact, obtaining commercial closed SWCNTs is quite difficult as these purification procedures are almost standardly used by many manufacturers, but essential as they serve as ideal reference standards for CNTs that cannot be filled. Of commercially available materials, high-pressure CO disproportion (HiPCo) method-produced SWCNTs (AP-HiPCo produced at Rice University or the AP grade of NoPo Nanotechnologies (NoPo), plasma torch synthesis (RN020 from Raymor Technologies), and electric-arc synthesis SWCNTs (AP grade from Carbon Solutions, Inc.), and non-commercial laser vaporization synthesis SWCNTs, have been reported to be dispersible with significant mass fractions of closed-ended SWCNTs.[4–11]

In the following, we give an overview of the two most commonly used procedures to open SWCNTs for subsequent filling.

Procedure 1: In a first step, all non-nanotube carbon species present in the samples, including the graphitic carbon shells around the catalytic particles are removed by air oxidation, thereby

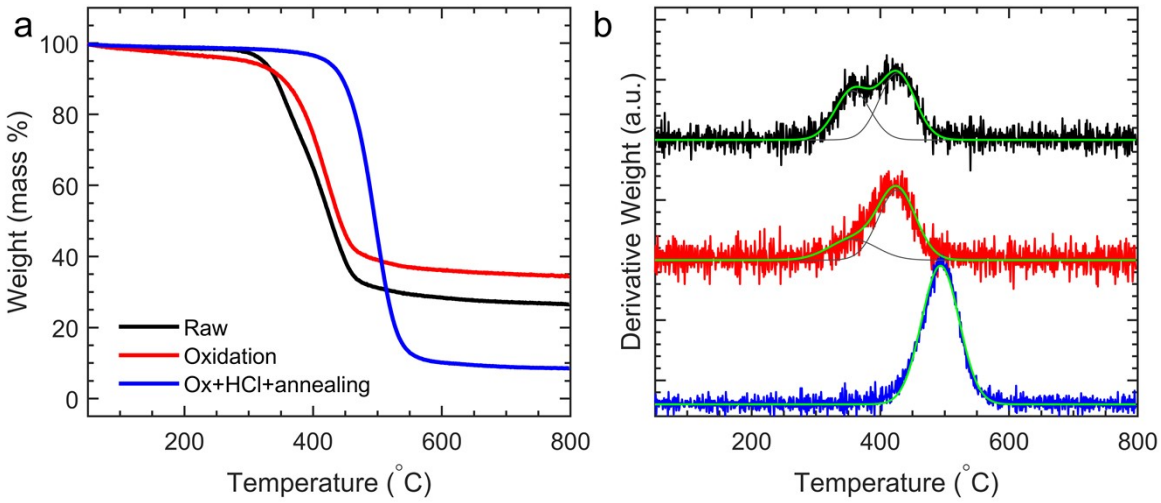

Figure S1: (a) TGA and (b) derivative-TGA (DTGA) curves of AP-grade Carbon Solution arc-discharge CNTs, as purchased (black), after air oxidation (red) and after air oxidation, acid treatment and annealing.

exposing the metal particles and SWCNTs for the subsequent processing steps. To define the oxidation temperature that needs to be used, as well as the weight percentage of the material that needs to be burned, thermo-gravimetric analysis (TGA) of the SWCNT powder can be performed. Typically, a TGA curve of raw SWCNT powders will contain two or more weight-loss peaks, with the highest temperature peak corresponding to the SWCNTs, and the lowest temperature peaks corresponding to the other carbonaceous materials present in the sample. A temperature is then chosen low enough to not harm the SWCNTs and sufficiently high to remove all other carbonaceous species. Figure S1 presents an example of a TGA analysis for the raw AP-SWCNTs from Carbon Solutions Inc.[12] By fitting the derivative of the TGA curves (DTGA, panel (b)) of the raw AP-SWCNTs from Carbon Solutions, Inc., it was found that they contain about 43% of SWCNTs that are burned at 426°C, 27% of catalytic particles and all other carbonaceous species burn at lower temperature. To remove all non-SWCNT carbonaceous species, an oxidation temperature of 350°C is chosen and the time for the oxidation was chosen until 30% weight loss was achieved. Similarly, for Raymor Arc-discharge SWCNTs (batch no. RNL 12-010-113), an oxidation temperature of 460°C and 55% weight loss has been previously employed to open the SWCNTs, and for HiPco SWCNTs (Carbon Nanotechnoligies Inc., batch P0279° an oxidation temperature of 375°C was employed.[9,13,14]

After this air oxidation step, the remaining SWCNT powder is treated ultrasonically for 1 hour (bath sonicator) in concentrated (37%) HCl at 60°C to disperse the catalytic nanoparticles and remove them by vacuum filtration as well as to open the SWCNTs through the sonication. Indeed, by monitoring the presence of the catalytic particles by TGA and electron paramagnetic resonance spectroscopy,[12] it was found that a large fraction of the catalytic nanoparticles is removed in this acid step and only a small fraction of less than 10wt% still remains (blue curve in Figure S1). Afterwards the SWCNTs are neutralized by excessive rinsing with deionized water and vacuum filtration over a 5µm polycarbonate filter.

In a final step, the so-obtained powder is annealed in high vacuum at 800°C for at least 1 hour to remove any residual functional groups which can block the SWCNT ends, as well as to remove any molecules (*e.g.* acid, water) from the SWCNT interior. Note that annealing at higher temperatures is unadvisable since this is shown to reclose the SWCNT ends. The annealing also results in more stable SWCNTs that now only burn at about 493°C (blue curve in Figure S1, showing now a mass percentage of 91% SWCNTs).

Procedure 2: Typically, 20 mg of raw SWCNT material is sonicated in nitric acid (35 vol %) (150 mL) with a sonic bath (160 W max) (100% for 5 min and then 40% for 15 min) and then heated at 100°C for 5 h.[15] The suspension is then cooled and vacuum-filtered through a PTFE membrane (Sartorius, 0.2 μm). While pursuing vacuum filtration, the thick SWCNT layer formed on the filtration membrane (buckypaper) is washed by 200 mL of deionized water while monitoring the pH during the washing and washing cycles were repeated until the filtrate is neutral. The nanotubes are redispersed in NaOH (1 M, 100 mL) using the sonic bath (100% for 10 min) and then filtered through a PTFE membrane and washed with 1 M NaOH, deionized water, and then 1 M HCl followed by deionized water until the filtrate was neutral. Finally, the buckypaper is redispersed in hydrogen peroxide (30%) (150 mL) using the sonic bath (100% for 5 min and then 40% for 10 min). The suspension is heated at 100°C for 1 h, cooled down at room temperature, and then vacuum-filtered through a PTFE membrane. The nanotubes are washed by 200 mL of deionized water and then dried at 50°C under high vacuum. The overall yield of the purification process is typically about 60% (12 mg).

BNNT opening: For opening BNNTs, the BNNT powder is annealed at 800°C in air for 2 hours, then sonicated in DMF using a cup sonicator until complete dispersion is observed. The solution is then centrifuged at 12,000g and the top half of the centrifuge tube is collected. The opening of the BNNTs occurs during the sonication step. An alternative way to open BNNTs is to apply mechanical grinding using a fine manual mortar.[16]

S1.2 Different filling procedures for CNTs ad BNNTs

Throughout the years, different strategies have been followed to fill SWCNTs with various compounds. In particular, liquid- and vapor-phase filling have been successful for the filling of SWCNTs with organic molecules. Besides the obvious choice for the correct SWCNT batch with corresponding inner cross-sectional diameter, the choice of filling procedure is strongly depending on the solubility, melting and sublimation point of the specific molecules in combination with their decomposition temperature.

Vapor-phase filling: which was originally used to fill C_{60} inside SWCNTs,[17] is typically performed as follows: SWCNTs and organic molecules are both put in a quartz T- shaped tube, but separated from each other at the two ends of the T-shape. The quartz tube is pumped to a high vacuum (typically ~10-6 mbar) and the SWCNT part is heated for a few hours up to 2 days at 300-400°C to outgas the SWCNTs, while keeping the organic molecules at room temperature in this process. After cooling, SWCNTs and organic molecules are then mixed (*e.g.* with a weight ratio around $m_{CNT}/m_{molecule}$=0.5), the glass vessel is sealed, so that the blend is now under static high vacuum (Figure S2 for an example of quaterthiophene molecules). The sealed glass vessel is put for several hours up to two days into a furnace at a temperature slightly above the sublimation temperature of the dye molecules.[18] As an example, typical temperature for quaterthiophene molecules is around 350°C[15,19,20] and for phthalocyanine molecules around 550°C.[21] After this encapsulation process (Figure S2), a second heating treatment can be performed, but under dynamic vacuum in order to remove the dye molecules in excess, stacked at the outer surface of the NT and/or the hybrid nano-systems can be washed several times with solvents in which the dye molecules can be solubilized in order to remove the remaining molecules from the outside of the SWCNTs.

Liquid-phase filling yields an alternative route to filling in case the sublimation temperature and decomposition temperature of the organic molecules are too close so that the molecules cannot be encapsulated through vapor-phase filling. In this method, the SWCNTs and organic molecules are both dispersed in a solvent which is then refluxed under inert atmosphere for several hours up to several days.[8,10,22–24] The choice of solvent is critical. Indeed, to obtain a complete filling of the SWCNTs, preferably a saturated solution of the organic molecules should be prepared, as it has been shown that at low concentrations, only partial filling can be achieved.[24] The procedure is then followed by repeated rinsing with a solvent in which the dye dissolves easily, over a filtration membrane with short batch sonication in between the subsequent washing cycles to remove any excess dye adsorbed on the outer SWCNT walls, similarly as applied for the vapor-phase filling. While liquid-phase filling has the major advantage to be applicable to any organic molecule, the main disadvantage includes that also the solvent molecules can be encapsulated, while in the vapor-phase filling this can be avoided.

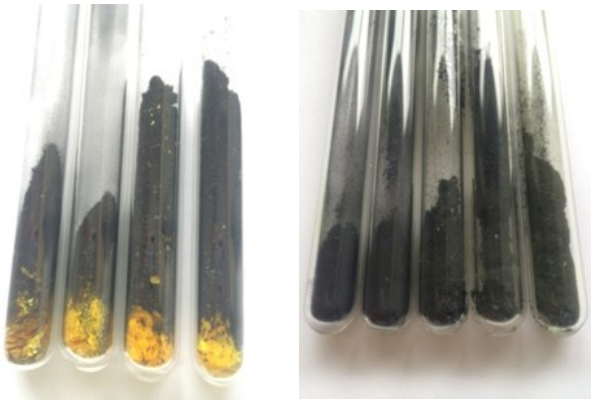

Figure S2: (left) Blend of dye molecules (yellow powder) and SWCNTs (black powder) before the temperature treatment. (right) Blend after heating under static high vacuum.

Filling by nano-extraction using supercritical CO_2: Supercritical CO_2 can be used as a solvent to perform a liquid-phase filling as described above. The main advantage of using supercritical CO_2 however, is that after the procedure, the CO_2 evaporates and solvent-filling can thus be avoided. Moreover, the system does not require high temperatures which could decompose the molecules of interest to be encapsulated, and molecules don't need to be soluble in a particular solvent as is required for the liquid-phase filling.[25–28] Typically, the reaction is carried out in a thermostated stainless steel reactor at a temperature of about 55°C and a pressure of about 150 bar. Pre-opened SWCNTs and molecules, *e.g.* fullerenes, are added in a 1:1 mass ratio. Before opening the reactor is cooled down and pressure is reduced to remove the CO_2. Afterwards, a similar washing procedure needs to be applied to remove excess unencapsulated molecules.

For BNNTs, similar techniques are performed to fill them with organic molecules.[16,29]

S1.3 Different procedures for externally functionalized NTs

As mentioned in the main text, the immobilization of molecules on the CNT surface can be achieved using different methods, that can be subdivided into non-covalent functionalization or covalent functionalization. In the following, two methods will be described to functionalize the CNT surface, the micelle-swelling approach and a covalent functionalization strategy that preserves the π-conjugation of the SWCNT wall. For other strategies, such as sp^3-functionalization we refer to other recent review papers.[30,31]

S1.3.1 Micelle-swelling approach

For non-covalent functionalization, one could, similarly as for liquid-phase filling, mix the SWCNT powder and the organic molecules in a solvent, reflux it or leave it stirring at room temperature. In case the SWCNTs are closed or have a too small diameter to encapsulate the molecule, the molecule will be adsorbed on their outer walls.[32] Additionally, also a dedicated linker molecule, such as pyrene, can be added to stabilize the SWCNT interaction.[33] A subsequent washing cycle can be performed to remove excess molecules, however with the complexity that such a washing can also remove the adsorbed molecules again. Therefore, this method is not generally applicable to any type of molecules and lacks a control over the functionalization efficiency. The so-called micelle-swelling approach[34] can be used instead, which is generally applicable for many molecules, does not require difficult chemistry routes and moreover can nicely control the stacking density on the SWCNT surface. In this approach, SWCNTs are first solubilised in an aqueous suspension with surfactants. The molecule of interest is dissolved in a solvent that is immiscible with water, after which it is added to the SWCNT suspension and mixed. The organic solvent containing the molecule will then start to penetrate the micelle and bring the molecule close to the SWCNT surface. Then, the solvent will evaporate (at slightly elevated temperature) while the molecules remain within the micelle core and stack themselves around the CNTs. As discussed in detail in section 2.2 in the main text, the SWCNT stacking density can be nicely controlled by the amount of solvent added and the concentration of the molecule in the solvent as well as by playing with the surfactant concentration,[35] as such capable of grafting many different molecules with largely varying and tuneable densities on the SWCNT sidewalls.[36–38]

S1.3.2 Covalent functionalization

The covalent method described in this section,[39] unlike most of the covalent approaches, does not change the hybridization status of the carbon atoms on which the functional groups are attached to. The carbon atoms below the attached groups keep their sp^2 character without affecting the extended π-conjugation of the SWCNT sidewalls, instead of being converted in their sp^3 form and into excitonic traps (see Figure S5a,b). To achieve this, the method relies on cycloaddition chemistry, which occurs exclusively between π-electrons. This strategy deploys cyanuric chloride (1,3,5-trichloro triazine); under the proper conditions, the triazine is converted into a highly reactive azido-derivative and attaches onto the SWCNTs sidewalls through a nitrene bridge, see [39] for the details. Favoured by the curvature of the tubes' sidewalls, the in-plane sigma carbon-carbon bond below the nitrene bridge is released and the two carbon atoms sustaining the functional group are in their sp^2 state (see Figure S5b). The reaction proceeds spontaneously, without an activation barrier. The temperature at which the reaction is performed affects the number of groups attached onto the SWCNTs sidewalls, making it a very efficient controller to tune the functionalization to very low (one triazine group every thousand carbon atoms) up to very high concentrations (one triazine group every 25 carbon atoms, for an effective functionalization ratio of 4%). The other two chlorine atoms of the triazine can also be easily replaced after the attachment onto the tubes, providing the capability of post-functionalization attachment of additional species onto the tubes. As an example, Godin and coworkers[40] conjugated the molecular switch spiropyran-merocyanine onto the triazine groups to gain control on the blinking dynamics of the SWCNTs.

S2 Evidence of 1D Heterostructures: a benchmark of techniques.

Full characterization of these complex hybrid systems can only be provided by using a wide range of dedicated experimental techniques, as not a single technique exists that can provide a complete picture. Even more importantly, a proper set of reference samples needs to be designed and compared to. The most essential characterization methodologies for each of the different functionalisation strategies are reviewed below, while mostly focusing on the main information that can be obtained from the different techniques.

S2.1 Reference Samples

S2.1.1 Endohedrally functionalized NTs

A key element in the characterization of SWCNT nanohybrids is the preparation of a proper set of reference samples. When spectroscopically characterizing filled SWCNTs (filler@SWCNT), at least the following reference samples should be prepared and compared with:

(1) **Empty SWCNTs**: In particular for endohedral hybrids, closed and therefore empty SWCNTs are extremely important reference samples (as the primary reference point for spectral positions etc.), which can, be prepared through careful solubilisation in aqueous suspensions (without using any sonication) of raw, as-synthesized SWCNTs[4] or using shear-force mixing[41] and subsequent separation by density gradient ultracentrifugation (DGU).[42,43]

(2) **Empty, but treated SWCNTs**: as discussed above, even more important is to prepare a sample in the same way as the filler@SWCNT samples, but starting from closed (non-opened) SWCNTs. When preparing a suitable start sample of predominantly closed tubes is difficult, also a mixture of empty and filled tubes can be used that is separated afterwards (after the filling procedure) by DGU into closed (empty) and opened (filled) SWCNTs.[14]

(3) **solvent@SWCNTs**: A sample of the same opened SWCNTs that has underwent the exact same preparation procedure except for the addition of the filled molecules, and thus may be filled with water or any solvents used during preparation and/or solubilization.

(4) **Free filler molecules in solution**, at least if soluble in the same solvent.

The preparation of such reference samples is detailed in the following:

First of all, when filling pre-opened SWCNTs with a particular molecule and afterwards dispersing the supposedly filled SWCNTs in an aqueous suspension, *comparison to both empty (non-filled) and water-filled SWCNTs* is essential. Indeed, when the pre-opened SWCNTs are not being filled with the molecule of choice, they will be most definitely filled with water during the aqueous dispersion, as it has been shown previously that water even spontaneously enters the smallest SWCNT diameters observed.[6] Comparing the filler@SWCNT samples with the water-filled SWCNTs in optical spectroscopy, can then be used to determine if the filler molecules are encapsulated.[8,9,14] This comparison can also be used to determine a minimal encapsulation diameter for the ‘filler’ molecule. Indeed, if the diameter is too small for the

'filler molecule', the SWCNT will be filled with water, while for larger diameters they will be filled by the 'filler molecule'. [8,9,14]

Secondly, when filling SWCNTs with chromophores, one needs to ensure that only encapsulated molecules are present and that molecules adsorbed on the outside of the SWNTs are entirely removed. This removal can be performed in a very drastic manner, by embedding the encapsulated SWCNTs in a piranha solution,[44] but is mostly done by repeatedly washing the SWCNTs with a solvent in which the chromophores dissolve easily.[9,10,14,23,45] Care must be taken to not extract the filler molecules through this procedure. For some filler molecules this was found to be more difficult (*e.g.* water or C_{60} are hard to re-extract once inside the SWCNTs) than for others, but often one needs to find the delicate balance between sufficiently thorough removal of the externally adsorbed molecules and not too much leaching of the encapsulated ones.[46] To optimize the washing cycles, one can perform the entire filling procedure from a SWCNT sample in which both closed and opened SWCNTs are present. Afterwards, the closed and opened SWCNTs can be separated by DGU and their optical spectra can be compared.[14] The closed SWCNTs can of course not encapsulate the molecules, and the washing procedure can hence be evaluated based on these closed SWCNTs not having any chromophores associated to them.

Finally, during any filling procedure, solvents are used to for example wash the excess of externally adsorbed molecules, and one cannot ignore that these solvents could also fill up the SWCNTs, and even replace the encapsulated species in the SWCNTs. Therefore, it is essential to prepare reference samples that are prepared in the same manner as the 'filler'@SWCNT samples, but without adding the filler. For example, repeating the washing procedure with pre-opened SWCNTs that are not exposed to the 'filler' molecule.

Importantly, it was previously observed that when using polymer wrapping in organic solvents (such as toluene) instead of aqueous suspension with surfactants, encapsulated chromophores that are soluble in the organic solvent can leak out of the SWCNTs.[14] Using aqueous suspensions with surfactants, this was never observed, most likely since the surfactants could block the ends of the SWCNTs or since most organic molecules have very low solubility in water. This is important to consider when characterizing nanohybrids in different environments.

S2.1.2 Exohedrally functionalized nanohybrids

When functionalizing SWCNTs through exohedral adsorption on their exterior walls, most important reference samples to consider are 'bare' SWCNTs, processed in a similar manner but without externally adsorbed molecules, that can serve as ideal reference samples for ruling out effects of filling of the SWCNTs with solvents used during the aggregation process (*e.g.* the solvent used during the micellar swelling approach). If using aqueous surfactant dispersions, a second important reference sample that needs to be prepared is one consisting of the chromophores added to a surfactant solution without the SWCNTs, yielding "free" chromophores dispersed in surfactant micelles. The latter ideally suits as a reference sample for non-interacting chromophores that could be present in the nanohybrid sample, and can also be helpful to estimate the PL quantum yield of the chromophores in different environments. In

many works, a sample of the dissolved chromophores in an organic solvent is additionally prepared, to compare to, in particular important since PL quantum efficiencies of the chromophores in organic solvents can be most accurately determined (since concentrations can be more accurately determined). In reference [35], a detailed investigation is performed on the effect of the chosen surfactant and added molecule concentration in the micelle-swelling approach. We realize such studies are extremely time-consuming and hence cannot be performed as a standard methodology for any other externally adsorbed chromophore, however, they yield extremely valuable information on how to optimize the functionalized hybrid structure: for example optimize the hybrids to a full coverage along the length of the SWCNTs while having a minimal amount of non-interacting chromophores in the suspension.

S2.2 Absorption Spectroscopy

S2.2.1 Endohedrally functionalized NTs

After functionalisation and dispersion of the nanohybrids, a quick ensemble overview of the content of the samples can be obtained by absorption spectroscopy. When comparing with the absorption spectra of empty, water- and/or solvent-filled SWCNTs (whenever solvents are involved in the preparation or solubilisation of the hybrid samples) and the reference samples discussed above, one can get information on (1) the presence of the chromophores (and, in combination with the above mentioned reference samples using closed tubes, also providing a first indication of encapsulation), (2) the changes of the SWCNTs optical transitions due to interaction with the filler (E_{11} being generally most sensitive to these effects[7–9,14,23,45], see e.g. also Figure 2-9) and (3) changes in the filler absorption band due to intermolecular interactions (*e.g.* in specific 1D stacking) and interaction with the SWCNTs.[9,10,14] For instance, Figure S3 presents the absorption spectra of squarylium@SWCNT hybrids as compared to the absorption

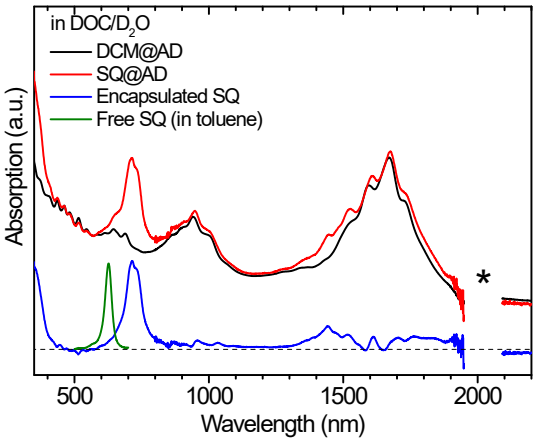

Figure S3: Absorption spectra of squarylium-filled arc-discharge SWCNTs (SQ@AD, in red) dispersed in an aqueous surfactant solution in sodium deoxycholate (DOC) in D2O compared to the absorption spectrum of the reference sample (dichloromethane filled: DCM@AD, in black). After subtracting the two absorption spectra from each other, the absorption spectrum of the encapsulated SQ dye can be obtained (difference spectrum in blue) and compared to the absorption spectrum of the SQ dye freely suspended in toluene. Figure adapted from reference [14]

spectra of a reference sample treated in the exact same manner but without bringing it in contact with the dye, and hence filled with the solvent used in the filling procedure, in that case dichloromethane. Comparing the absorption spectra and in particular making the difference spectrum (shown in blue in Figure S3) clearly indicate the presence of the dye. In addition, when comparing the absorption spectrum of the encapsulated dye with that of the free dye in solution, a clear shift of up to ~100 nm can be observed indicative of a different interaction of the dyes with their environment (in this case proven to originate from a J-aggregate like stacking of the molecules inside the SWCNTs).[14] This becomes even more evident when subsequently sorting the SWCNTs.[10] Also in this case, the shifts of the electronic transitions of the SWCNTs can be a direct proof of the different filling of the SWCNTs. Direct proof of encapsulation as opposed to exohedral functionalisation comes from comparing samples prepared using closed and opened SWCNTs.

Doping of SWCNTs can also be quantified by absorption spectroscopy, through the suppression of the 1st (and subsequently higher-order) van Hove transitions of the SWCNTs.[18,47,48] Even charge manipulation of encapsulated beta-carotene molecules inside SWCNTs has been demonstrated, using electrochemical doping techniques, showing that electrons could be extracted from the encapsulated molecules when the external electrochemical potentials were shifted.[48]

Finally, absorption spectroscopy is also essential to calibrate and compare PL quantum efficiencies (of the encapsulated dyes and the SWCNTs), as presented further on.

S2.2.2 Exohedrally functionalized NTs

Similar as for endohedral hybrids, absorption spectroscopy will yield direct information on the effect of the interaction by shifts and line width changes of both the chromophores and the SWCNTs optical transitions and is extremely helpful in estimating the amount of non-

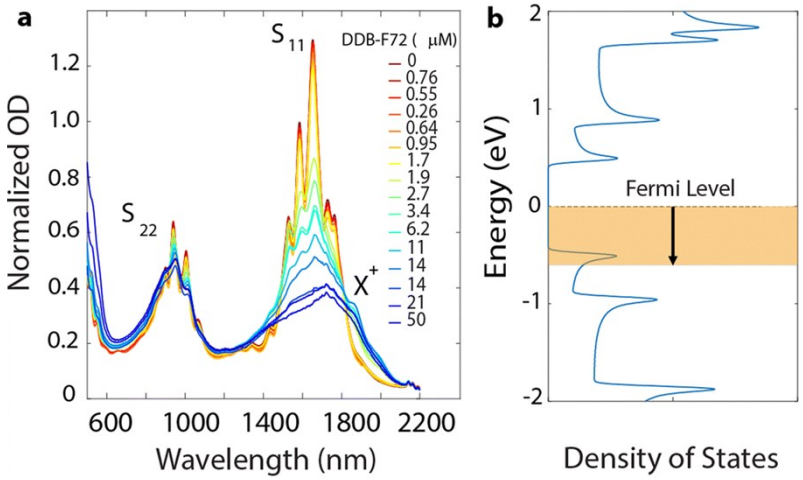

Figure S4: (a) Absorption spectra of SWCNTs doped with different concentrations of non-covalently adsorbed dodecaborane clusters (DDB-F72) with the dark red trace representing the undoped sample and the dark blue trace representing a highly doped sample. A new absorption peak related to the trion X^+ is also shown at around 1850 nm. (b) Fermi energy shift due to molecular doping, showing the DOS of a (10,8) chirality. Figure reproduced from reference [47]

interacting chromophores (through the fact that those don't show a shifted absorption spectrum with respect to the corresponding reference samples, see for example Figure 2-5). If assuming the absorption cross-sections of the chromophores (or CNTs) do not change significantly upon functionalisation, which is generally a reasonable approximation, the number of adsorbed molecules can be estimated from the relative intensity of the SWCNT and chromophore absorptions. As such, optical absorption spectroscopy becomes a quantitative technique, and can even be used to access the absorption cross-section of the SWCNTs through that of the adsorbed molecules.[49] Note that doping of SWCNTs through exohedral functionalisation yields the same effect on the SWCNT optical properties as for the endohedral hybrids, as presented in Figure S4.[47]

S2.3 (ensemble) NIR Photoluminescence-Excitation Spectroscopy (PLE)

In PLE spectroscopy, the emission of semiconducting SWCNTs can be mapped out versus the multiple higher energy excitation bands, thereby resolving each semiconducting chirality in a bulk sample.[50] PLE spectroscopy is therefore an extremely important technique to characterize nanohybrids composed of semiconducting SWCNTs, in particular when combined with detailed fitting of the resulting experimental data, so that shifts in emission and excitation energies, changes in line widths and intensities and the appearance of new features such as energy transfer peaks can be accurately extracted from the wavelength-dependent PLE maps.[8,10,14,35,49,51]

As explained in the main text, filling of SWCNTs results in shifts of the electronic transitions of the SWCNTs (Figure 2-7), as well as a broadening of the line widths and a reduction of the PL quantum efficiency of the SWCNTs.[8,11] These electronic shifts and line broadenings appear to be characteristic for the molecules that have been encapsulated[8], and are even sensitive to changes in the molecular arrangement of the encapsulated molecules, revealing *e.g.* phase transitions (Figure 2-8).[52,53] Comparing the electronic peak positions of SWCNTs filled with a particular molecule, with the peak positions of the above mentioned reference samples, it is even possible to determine a minimal encapsulation diameter, as shown in Figure 5-5.[9] For chromophore-filled SWCNTs, energy transfer can be observed as additional peaks appearing in the PLE maps, corresponding to excitation of the encapsulated dye, followed by transfer of energy to the SWCNTs and emission from the SWCNTs, from which detailed information can be deduced on the minimal encapsulation diameter as well as the specific stacking of molecules inside the SWCNTs (see Figures 4-4 and 4-5).[10,14] Also for doped SWCNTs, by charge transfer from the encapsulated species or by covalent functionalisation, PLE can be very useful, to *e.g.* determine the changes in PL quantum efficiency (Figure 4-2) as well as the occurrence of new emission peaks, originating from the formation of trions.[54,55] Moreover, covalent sp^3-functionalisation of SWCNTs can also result in new emission peaks, due to defect-induced trapping of excitons on the SWCNTs.[30,56,57]

Similarly, exohedral functionalisation can lead to very efficient and complete energy transfer of the adsorbed molecules to the SWCNTs,[49,51,58] previously employed to determine the chirality-dependent absorption cross-section of SWCNTs.[49]

Interestingly, while PL quantum efficiencies of molecules adsorbed on or encapsulated in SWCNTs are typically quenched completely, molecules@BNNTs remain highly fluorescent, and the shifts and changes in the emission spectra of the encapsulated molecules can also be used to evidence molecules are encapsulated[16], especially when combined with fluorescence anisotropy measurements.[29]

S2.4 Resonant Raman Scattering (RSS)

Arguably the most powerful spectroscopic technique when it comes to characterizing molecular filling of SWCNTs is resonant Raman spectroscopy (especially when using multiple laser wavelengths to probe many chiralities).

The first reason is that the ***radial breathing modes*** (RBMs) of SWCNTs are very sensitive to the additional restoring force exerted by a filler, causing an upshift of the RBM frequency. When SWCNTs are dispersed in bile salt surfactants (*e.g.* sodium deoxycholate),[4] the homogeneous steroid coating ensures that these RBMs have very narrow linewidths, allowing for RBMs of empty and filled SWCNTs to be clearly distinguished (and this separately for each chirality; see Figures 5-5b and 5-5c), and enabling trends in the diameter-dependent stacking to be discerned from the chirality dependent variation in the size of the RBM shift, *e.g.* providing a minimal encapsulation diameter (Figure 5-5d).[6,8,9]

A second reason to use RRS for characterizing filled SWCNTs is that the ***G-band*** and ***D-band*** are sensitive to doping that may arise through charge transfer between the filler and encapsulating SWCNTs (Figure 4-1).[20] Aryl-based chemistry (and analogue covalent routines, as sketched in Figure S5a) covalently attaches a desired group onto a single carbon atom, converted into its sp^3 state[59]). In this framework, Raman spectroscopy is a powerful tool to monitor and quantify the outcome of the process, since the D-to-G band ratio reflects the fraction of sp^3 carbon atoms within the sp^2 network.[60] This is not the case for the triazine-based

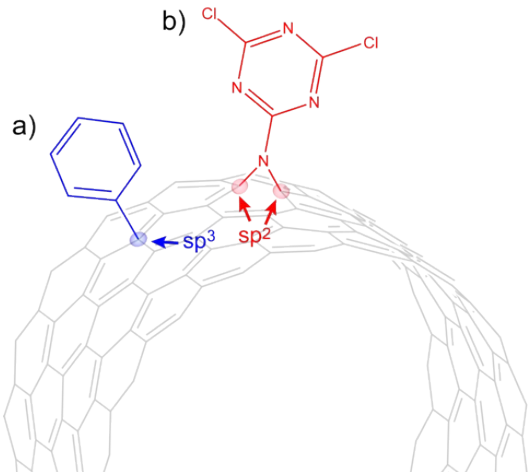

Figure S5: (a) Comparison between the sketch of aryl- (a) and triazine-functionalized carbon nanotubes (b) Please note the different hybridization states of the carbon atoms sustaining the functional groups in both compounds. [59,39]

covalent functionalization scheme, where the functional group is covalently linked to two nearby-lying carbon atoms, both in their sp^2 state as sketched in Figure S5b).

RRS can also be used to probe the ***Raman spectra of the encapsulated species*** themselves. A major advantage here is that the fluorescence of encapsulated molecules (which often forms a prohibitively strong background for resonant Raman measurements on free organic molecules in solution) is generally drastically quenched by the SWCNTs, and that the J-aggregate like assemblies of encapsulated molecules combine a large number of molecules totalling into a huge total Raman cross-section.[61] This yields Raman intensities that are even very promising for using single filled SWCNTs as Raman probes for multispectral bio-imaging.[61]

RRS becomes even more powerful when performed as a 2D spectroscopic technique with continuously tunable laser wavelength. The obtained 2D Raman-excitation maps allow not only all individual chiralities and their electronic transitions to be discerned through their different RBM frequencies and electronic resonances,[62–65] but also to distinguish different encapsulated species with different electronic transitions and vibrational signatures. This has for instance been used to characterize vibrational and electronic effect of water-filling of SWCNTs,[5,6] the vibrational[66] and electronic resonances (hence band gap)[67,68] of linear carbon chains (carbyne) synthesized inside DWCNTs, even at the single tube level,[69] and of graphene nanoribbons synthesized inside SWCNTs.[70]

S2.5 Single nanotube PL and Raman Characterization

While ensemble PLE and Raman spectroscopy provide an averaged view on the novel functionalities of the nanohybrids and can in some cases yield information on the filling efficiency or specific stacking of the molecules inside, more detailed information can be obtained when applying these techniques on the level of individual SWCNTs.

As a first example, Heeg *et al* demonstrated with tip-enhanced Raman spectroscopy (TERS) on individual LCC@DWCNTs that the specific Raman frequency of a linear carbon chain encapsulated in different CNTs does not depend anymore on the length of the chain, the latter being simultaneously available through the TERS mapping, but depends strongly on the specific diameter of the CNT surrounding the LCC.[66] This observation was not possible with ensemble spectroscopy, where different vibrational frequencies and bandgaps of the encapsulated chains where observed, but could not be related to their length nor to the specific surrounding CNT diameter.[68,71] Hence, these single-nanotube studies allowed for linking the structural information of the chains and surrounding CNTs to the specific optical and vibrational properties. TERS was also useful to provide evidence of partial filling of the LCCs in the DWCNTs, with alternating empty and filled sections[72], while ensemble Raman spectroscopy might have given the wrong impression of very high filling efficiencies due to the very high intrinsic Raman cross-section of the encapsulated chains.[73]

Plasmonic enhancement through positioning of specific mol@CNT hybrids in between a gold plasmonic dimer used for surface-enhanced Raman scattering (SERS) resulted not only in an extreme enhancement of the Raman signals of the 6T@CNT sample (estimated to be of the order of 9×10^4, but also allowed to investigate the orientation of the molecules within the CNT through polarization-dependent measurements.[74]

Even without the plasmonic enhancement, polarization-dependent single-nanotube Raman or PL spectroscopy allow to visualize the orientation and self-organization of molecules on the outside[75] or inside[44] of the SWCNTs and BNNTs.[29] Such polarization-dependent studies can thus provide ordering of the molecules inside the NTs, in a complementary way to high-resolution transmission electron microscopy.

Finally, the functionalization of CNTs with molecules can also result in novel properties of the hybrids for bio-imaging applications and sensing. For example, SWCNTs functionalized through covalent functionalization with spiropyran switches have demonstrated to be ideally suited for super-resolution PL microscopy, as a consequence of their ability to blink under UV light through photoswitching of the spiropyran to merocyanine.[40] This allows the unique narrowband NIR emission of the SWCNTs that is overlaying with the NIR biological transmission windows to be exploited for in vivo super-resolution imaging in cells.[40]

Finally, functionalisation of SWCNTs with single-stranded DNA segments or other biocompatible polymers has provided new avenues towards single-nanotube biosensing applications with high sensitivity, high specificity and possibility for in vivo characterization.[76–80]

S2.6 Time-resolved spectroscopy

As discussed already in detail in the main manuscript in section 4-2, time-resolved spectroscopy can be used to investigate in depth the mechanism and dynamics of the energy or charge transfer between encapsulated/adsorbed molecules and NTs. Interestingly, for CNT-hybrids, time-resolved emission spectroscopy and transient absorption spectroscopy can get access both to the excited state dynamics of the molecules and the CNTs. For example, water-filled SWCNTs were found to exhibit overall slightly shorter lifetimes of their excited states compared to empty SWCNTs,[11] while external functionalisation can either lead to much longer timescales of the SWCNT emission, either by localisation of the charges in quantum defects or through triplet sensitization causing delayed fluorescence.[31,81–83] Time-resolved emission spectroscopy of the encapsulated or adsorbed molecules typically shows significantly reduced lifetimes of the molecules leading to severe quenching of the molecule steady-state emission.[14,32,84,85] However, very often, a small minority of non-adsorbed molecules is still present in the sample, leading to multi-exponential lifetimes with both short and longer living components.[85,86]

Transient absorption spectroscopy on the other hand can study the population build-up of excitons on the SWCNTs after optical excitation of the surrounding (*e.g.* porphyrins[58]) or encapsulated molecules (*e.g.* squaraine dye[14]), typically occurring within a time scale shorter than 100fs, essentially showing ultrafast and highly efficient[87] energy transfer from the molecules to the SWCNTs (as described in detail in section 4-2). Pump-probe spectroscopy is very useful in this perspective as both the dynamics of the molecule and the SWCNTs can be probed, after excitation of either of them. Similarly, with all other spectroscopic techniques, reference samples of the SWCNTs and molecules should be investigated separately to compare against.

S2.7 Electron Microscopy Techniques

The stabilization of the molecules inside the SWCNT offered a unique way to image and probe them, using in particular Transmission Electron Microscopy (TEM) and spectroscopies which have become essential tools over the time to study the structure of nanotubes and their hybrids.[88–90] The integration of aberration correction with reduced beam voltages (20-60keV) has facilitated atomic-level resolution of heterostructure configurations, circumventing damage and undesirable charge accumulation in dielectric compounds. Ongoing advancements in monochromators and energy filters have broadened the scope of investigation to encompass vibrational and electronic states within the 200 meV to few volts range, achieving unprecedented resolutions. These technical advances have been decisive for making possible the acquisition of images in HRTEM or STEM/HAADF modes in which atoms position and light impurity atoms such as C, B, N or O can be directly identified.[91–94]The latest generation of machines operated at low voltage have shown to be unmissable tools to reveal the presence of molecules filling the inner cavity of the tubes and inspect their 1D spatial organization.[90,95–97] Besides Electron Energy Loss Spectroscopy (EELS) has been widely used for decades to perform elemental analysis at a quantitative level with high spatial resolution, and to investigate dielectric losses in the 0 – 50 eV low loss range. Like absorption optical spectroscopies, EELS further allows the observation of electronic transitions,[98,99] with an energy resolution able to discriminate the spectroscopic response of the different components of an hybrid system such as molecule and tubes in which there are encapsulated,[16,19] the measurements of momentum q-dispersions of the excitations[100–102] as well as the study of vibration modes.[103] In the very recent years, EELS has greatly beneficiated from the emergence of new kinds of highly sensitive detectors.[104] Moreover, the emergence of next-generation direct fast cameras has amalgamated high dynamics with heightened sensitivity, furnishing the means to scrutinize atomic dynamics under beam exposure, temperature fluctuations, or under the influence of magnetic/electrical fields. New types of modes such DPC and STEM 4D based on this detector generation have open new avenues for investigating at a nm scale various physical properties and for mapping various fields such strain, deformation, polarization, charge transfer, electrical fields and magnetization with an unprecedented sensitivity.[105–109]

S2.8 Electron Paramagnetic Resonance spectroscopy (EPR)

Another technique which is very useful in specific cases is electron spin resonance (ESR) or electron paramagnetic resonance (EPR) spectroscopy, of course provided that paramagnetic species are involved. EPR spectroscopy has for instance been used to investigate the dynamics and deformations of fullerenes inside SWCNTs using fullerenes that were themselves endohedrally labelled with a nitrogen atom or transition metal paramagnetic probe, *e.g.* N@C_{60}@SWCNT[110,111] or La@C_{82}@SWCNT.[112] Also the interactions with the spins of the charge carriers on the SWCNTs themselves were investigated in this way. For paramagnetic organometallic molecules (in particular $Cu(acac)_2$) stacked as 1D arrays inside SWCNTs, EPR spectroscopy can provide detailed information on the orientation and spacing of the molecules.[46]

EPR spectroscopy using externally adsorbed cobalt porphyrin molecules as paramagnetic probes has been used to characterize the different interaction of the porphyrins with metallic and semiconducting SWCNTs,[32] which actually resulted in a quantitatively accurate method to determine the ratio of metallic to semiconducting tubes present in a bulk SWCNT sample.[86] The strength of this technique is its absolute accuracy, but not its sensitivity, i.e. it is probably the best spectroscopic method available to date to characterize the absolute metallic/semiconducting content of partially enriched samples from selective synthesis methods, but it would be difficult to detect the very small fraction of remaining metallic tubes in highly purified semiconducting SWCNTs (or vice versa) from today's state-of-the-art sorting methods. For the latter, wavelength-dependent Raman spectroscopy is probably most suitable.

S2.9 Other techniques

While many of the above techniques determine filling or external functionalisation through the effect of the encapsulated, attached or adsorbed molecule on the SWCNs' optical and electronic properties, the non-perturbing nature of the above mentioned triazine-based sp2-functionalization makes the tubes preserve their pristine properties, which, as a drawback, makes the quantification of the functionalization outcome very challenging.[39] Quantification of the functionalization outcome by all-optical means becomes thus very elusive: No increase of the D-to-G band ratio can be observed as compared to sp^3-functionalization[60] nor any onset of emission bands due to defect-activated trap- or dark-excitonic states.[59] The density of functional groups attached to the carbon nanotubes depends upon the incubation temperature of the triazine-containing solution in which the nanotubes are stirred during the preparation procedure. A temperature of 25°C yields 1% of functionalization (approximately one functional group each 100 carbon atoms), whereas an operational temperature of 70°C yields 4% of functionalization (one functional group each 25 carbon atoms). A multi-step characterization scheme needs to be thoroughly pursued to determine those compositions, since no direct all-optical evidence of the functionalization is possible. The first step requires thermogravimetric analysis to verify the covalent nature of the established bonds and rule out spurious supramolecular assemblies. The subsequent step requires elemental analysis and/or x-ray spectroscopy (in the C1s and N1s regions). Those two techniques independently recognize the composition and relative abundance of the different chemical species present within the samples, enabling a quantification of the density of functional groups attached onto the carbon nanotubes. X-ray spectroscopy, moreover, grants additional insight into the samples: It is for example able to distinguish between the two chemically different nitrogen species within the compounds, singling out the ones within the triazine ring from the one bridging the ring to the carbon atoms of the tubes (highlighted with a bold **N** in Fig. S5b). Those latter nitrogen atoms, fully integrated within the conjugated sp^2 network of the nanotubes, contribute with their electron lone pair to the density of electrons in the nanotubes, uplifting the position of the Fermi level of the tubes more and more when increasing the density of functional groups. Those shifts of the chemical potential within the tubes can be quantified by following the position of the sp^2 component of the C1s XP spectra of the compounds. Alternatively, monitoring the broadening

of the G^- band due to the longitudinal optical phonon in metallic nanotubes provides also an independent estimation of the shift of the Fermi level.

S3 Determining the percentage of filling

One of the essential questions when discussing filling of SWCNTs is how efficient the filling is and whether or not the SWCNTs are filled along their entire length. Ensemble RBM spectroscopy resolving the empty and water-filled SWCNTs present in a specific sample showed up to 100% intensity in the 'water-filled' RBM peaks for certain samples, indicating a complete filling of the SWCNTs.[5] Initial single-tube PL investigations on individual empty and water-filled SWCNTs measuring the shifted emission of water-filled SWCNTs along the length of the SWCNTs clearly showed that if a nanotube is filled, it is filled along its entire length with water, even if the SWCNTs are several micrometers long, provided the SWCNTs remain embedded in an aqueous environment.[11] However, since the exciton on the SWCNTs has a long diffusion length, hence probing a long section of the SWCNTs, and at the same time due to the limiting spatial resolution in such single-tube optical measurements, this cannot be used as a direct proof of complete filling. More recently, partial filling with n-hexane has been demonstrated by PL hyperspectral imaging spectroscopy along the length of an individual nanotube.[113] It was also confirmed for dye-filling through mapping the Raman spectrum of the dye inside ultralong SWCNTs, that SWCNTs more than 100µm in length, could be easily filled along their entire length.[24]

For water filling, a near-to complete close-packing geometry of the water molecules inside SWCNTs of any diameter was found through measuring the differences in density between the empty and water-filled SWCNTs.[114] For dye-filled SWCNTs, both thermogravimetric analysis and elemental analysis of the as-prepared nanohybrids demonstrated, by comparison with molecular models, a close to complete filling of the SWCNTs with dipolar organic dye molecules.[9] However, these destructive characterization techniques are quite wasteful and only applicable when sufficient sample quantities are available.

Indirect information of complete filling was obtained from the extremely large enhancement of the nonlinear optical effect of dipolar dyes inside the SWCNTs, attributed to their head-to-tail alignment (see section 5.2) can only be explained without the presence of interstitial solvent molecules, which would otherwise diminish the dipolar coupling between the dipolar dyes and hence prevent the alignment of 55-70 dyes in the same sense.[9] Also in the J-aggregated stacking observations for other dyes inside SWCNTs, such as the squarylium and sexithiophene dyes,[10,14,16,24,61] interstitial solvent molecules would not allow to observe the strongly shifted spectra of the encapsulated dyes due to the strong intermolecular coupling. Hence, optical spectroscopy, as well as TGA, elemental analysis and DGU separations all point towards a near-to-complete filling of the SWCNTs.

In HRTEM, lower filling efficiencies are typically found, with filled and empty sections along the length of the SWCNT. However, one should keep in mind that the filling factor depends on many physical interactions occurring at the ends of the nanotube for molecular entering but also inside the nanotube with competitions between molecular adsorption and molecular diffusion, presence of interstitial solvents or not, which all depend on thermodynamical

parameters and geometrical aspects of the nanotube and the molecule. Also the influence of the electron beam, even when using low doses, can also not be neglected, see *e.g.* the time-dependent twisting of graphene nanoribbons under the influence of an electron beam in reference [70].

The Raman signal from a carbon nanotube can also be used as a relative internal reference to compare the filling factor of different Mol@CNT or to compare different encapsulation methods. Note that, due to the huge resonance effects in both the CNTs and filled molecules response, this comparison must be done with nanotubes of the same chirality, the same molecules and the same excitation wavelengths. Using this method, it can be shown that the filling factor strongly depends on the thermodynamic parameters used for the filling process such as temperature and concentration.[24] As another example, it was commonly observed that vapour phase encapsulations of polythiophenes in carbon nanotubes (*e.g.* 6T, 4T) lead to higher ratio's of molecule / nanotube Raman bands, compared to liquid phase process, indicating a better filling factor.[15] This is probably due to the high temperature and vacuum process used for sublimating the molecules that enhances the thermodynamic encapsulation driving force.

Also for linear carbon chains synthesized within DWCNTs, it was observed through near-field tip-enhanced Raman spectroscopy that some parts of the DWCNTs are filled with the chains, while others are not, however, in this case the 'filling' procedure is entirely different, doing the synthesis within the SWCNTs making it logical that the efficiency could be much lower (see *e.g.* Figure 3-1).[66]

Overall, the fine understanding of the elementary filling process, the final filling factor, as well as the migration thermodynamics of molecules inside nanotube needs further experiments, at the single molecule and single nanotube scales.

References

(1) Yang, F.; Wang, M.; Zhang, D.; Yang, J.; Zheng, M.; Li, Y. Chirality Pure Carbon Nanotubes: Growth, Sorting, and Characterization. *Chem. Rev.* **2020**, *120* (5), 2693–2758. https://doi.org/10.1021/acs.chemrev.9b00835.

(2) Park, T.-J.; Banerjee, S.; Hemraj-Benny, T.; Wong, S. S. Purification Strategies and Purity Visualization Techniques for Single-Walled Carbon Nanotubes. *J. Mater. Chem.* **2006**, *16* (2), 141–154. https://doi.org/10.1039/B510858F.

(3) Shi, Z.; Lian, Y.; Liao, F.; Zhou, X.; Gu, Z.; Zhang, Y.; Iijima, S. Purification of Single-Wall Carbon Nanotubes. *Solid State Commun.* **1999**, *112* (1), 35–37. https://doi.org/10.1016/S0038-1098(99)00278-1.

(4) Wenseleers, W.; Vlasov, I. I.; Goovaerts, E.; Obraztsova, E. D.; Lobach, A. S.; Bouwen, A. Efficient Isolation and Solubilization of Pristine Single-Walled Nanotubes in Bile Salt Micelles. *Adv. Funct. Mater.* **2004**, *14* (11), 1105–1112. https://doi.org/10.1002/adfm.200400130.

(5) Wenseleers, W.; Cambré, S.; Čulin, J.; Bouwen, A.; Goovaerts, E. Effect of Water

Filling on the Electronic and Vibrational Resonances of Carbon Nanotubes: Characterizing Tube Opening by Raman Spectroscopy. *Adv. Mater.* **2007**, *19* (17), 2274–2278. https://doi.org/10.1002/adma.200700773.

(6) Cambré, S.; Schoeters, B.; Luyckx, S.; Goovaerts, E.; Wenseleers, W. Experimental Observation of Single-File Water Filling of Thin Single-Wall Carbon Nanotubes Down to Chiral Index (5,3). *Phys. Rev. Lett.* **2010**, *104* (20), 207401. https://doi.org/10.1103/PhysRevLett.104.207401.

(7) Campo, J.; Piao, Y.; Lam, S.; Stafford, C. M.; Streit, J. K.; Simpson, J. R.; Hight Walker, A. R.; Fagan, J. A. Enhancing Single-Wall Carbon Nanotube Properties through Controlled Endohedral Filling. *Nanoscale Horizons* **2016**. https://doi.org/10.1039/c6nh00062b.

(8) Campo, J.; Cambré, S.; Botka, B.; Obrzut, J.; Wenseleers, W.; Fagan, J. A. Optical Property Tuning of Single-Wall Carbon Nanotubes by Endohedral Encapsulation of a Wide Variety of Dielectric Molecules. *ACS Nano* **2021**, *15* (2), 2301–2317. https://doi.org/10.1021/acsnano.0c08352.

(9) Cambré, S.; Campo, J.; Beirnaert, C.; Verlackt, C.; Cool, P.; Wenseleers, W. Asymmetric Dyes Align inside Carbon Nanotubes to Yield a Large Nonlinear Optical Response. *Nature Nanotechnol.* **2015**, *10* (3), 248–252. https://doi.org/10.1038/nnano.2015.1.

(10) Forel, S.; Li, H.; van Bezouw, S.; Campo, J.; Wieland, L.; Wenseleers, W.; Flavel, B. S.; Cambré, S. Diameter-Dependent Single- and Double-File Stacking of Squaraine Dye Molecules inside Chirality-Sorted Single-Wall Carbon Nanotubes. *Nanoscale* **2022**, *14* (23), 8385–8397. https://doi.org/10.1039/D2NR01630C.

(11) Cambré, S.; Santos, S. M.; Wenseleers, W.; Nugraha, A. R. T.; Saito, R.; Cognet, L.; Lounis, B. Luminescence Properties of Individual Empty and Water-Filled Single-Walled Carbon Nanotubes. *ACS Nano* **2012**, *6* (3), 2649–2655. https://doi.org/10.1021/nn300035y.

(12) Cambré, S. Endo- and Exohedral Carbon Nanotube Hybrids: Preparation and Spectroscopic Characterisation, Univeristy of Antwerp, Belgium, 2008.

(13) Torres-Dias, A. C.; Cambré, S.; Wenseleers, W.; Machon, D.; San-Miguel, A. Chirality-Dependent Mechanical Response of Empty and Water-Filled Single-Wall Carbon Nanotubes at High Pressure. *Carbon* **2015**, *95*, 442–451. https://doi.org/10.1016/j.carbon.2015.08.032.

(14) van Bezouw, S.; Arias, D. H.; Ihly, R.; Cambré, S.; Ferguson, A. J.; Campo, J.; Johnson, J. C.; Defillet, J.; Wenseleers, W.; Blackburn, J. L. Diameter-Dependent Optical Absorption and Excitation Energy Transfer from Encapsulated Dye Molecules toward Single-Walled Carbon Nanotubes. *ACS Nano* **2018**, *12* (7), 6881–6894. https://doi.org/10.1021/acsnano.8b02213.

(15) Almadori, Y.; Alvarez, L.; Le Parc, R.; Aznar, R.; Fossard, F.; Loiseau, A.; Jousselme, B.; Campidelli, S.; Hermet, P.; Belhboub, A.; Rahmani, A.; Saito, T.; Bantignies, J.-L. Chromophore Ordering by Confinement into Carbon Nanotubes. *J. Phys. Chem. C* **2014**, *118* (33), 19462–19468. https://doi.org/10.1021/jp505804d.

(16) Allard, C.; Schué, L.; Fossard, F.; Recher, G.; Nascimento, R.; Flahaut, E.; Loiseau, A.; Desjardins, P.; Martel, R.; Gaufrès, E. Confinement of Dyes inside Boron Nitride Nanotubes: Photostable and Shifted Fluorescence down to the Near Infrared. *Adv. Mater.* **2020**, *32* (29), 2001429. https://doi.org/https://doi.org/10.1002/adma.202001429.

(17) Smith, B. W.; Monthioux, M.; Luzzi, D. E. Encapsulated C60 in Carbon Nanotubes. *Nature* **1998**, *396* (6709), 323–324. https://doi.org/10.1038/24521.

(18) Takenobu, T.; Takano, T.; Shiraishi, M.; Murakami, Y.; Ata, M.; Kataura, H.; Achiba,

Y.; Iwasa, Y. Stable and Controlled Amphoteric Doping by Encapsulation of Organic Molecules inside Carbon Nanotubes. *Nature Mater.* **2003**, *2* (10), 683–688. https://doi.org/10.1038/nmat976.
(19) Alvarez, L.; Almadori, Y.; Arenal, R.; Babaa, ||r; Michel, T.; Le Parc, R.; Bantignies, J.-L.; Jousselme, B.; Palacin, ^s; Hermet, ^p; Sauvajol, J.-L. Charge Transfer Evidence between Carbon Nanotubes and Encapsulated Conjugated Oligomers. *J. Phys. Chem. C* **2011**, *115* (24), 11898–11905. https://doi.org/10.1021/jp1121678.
(20) Almadori, Y.; Delport, G.; Chambard, R.; Orcin-Chaix, L.; Selvati, A. C.; Izard, N.; Belhboub, A.; Aznar, R.; Jousselme, B.; Campidelli, S.; Hermet, P.; Le Parc, R.; Saito, T.; Sato, Y.; Suenaga, K.; Puech, P.; Lauret, J. S.; Cassabois, G.; Bantignies, J. L.; Alvarez, L. Fermi Level Shift in Carbon Nanotubes by Dye Confinement. *Carbon* **2019**, *149*, 772–780. https://doi.org/10.1016/j.carbon.2019.04.041.
(21) Alvarez, L.; Fall, F.; Belhboub, A.; Le Parc, R.; Almadori, Y.; Arenal, R.; Aznar, R.; Dieudonné-George, P.; Hermet, P.; Rahmani, A.; Jousselme, B.; Campidelli, S.; Cambedouzou, J.; Saito, T.; Bantignies, J.-L. One-Dimensional Molecular Crystal of Phthalocyanine Confined into Single-Walled Carbon Nanotubes. *J. Phys. Chem. C* **2015**, *119* (9), 5203–5210. https://doi.org/10.1021/acs.jpcc.5b00168.
(22) Yanagi, K.; Miyata, Y.; Kataura, H. Highly Stabilized β-Carotene in Carbon Nanotubes. *Adv. Mater.* **2006**, *18* (4), 437–441. https://doi.org/10.1002/adma.200501839.
(23) Yanagi, K.; Iakoubovskii, K.; Matsui, H.; Matsuzaki, H.; Okamoto, H.; Miyata, Y.; Maniwa, Y.; Kazaoui, S.; Minami, N.; Kataura, H. Photosensitive Function of Encapsulated Dye in Carbon Nanotubes. *J. Am. Chem. Soc.* **2007**, *129* (16), 4992–4997. https://doi.org/10.1021/ja067351j.
(24) Gaufrès, E.; Tang, N. Y. W.; Favron, A.; Allard, C.; Lapointe, F.; Jourdain, V.; Tahir, S.; Brosseau, C.-N.; Leonelli, R.; Martel, R. Aggregation Control of α-Sexithiophene via Isothermal Encapsulation Inside Single-Walled Carbon Nanotubes. *ACS Nano* **2016**, *10* (11), 10220–10226. https://doi.org/10.1021/acsnano.6b05660.
(25) Cadena, A.; Botka, B.; Székely, E.; Kamarás, K. Encapsulation of Sexithiophene Molecules in Single-Walled Carbon Nanotubes Using Supercritical CO2 at Low Temperature. *Phys. status solidi* **2020**, *257* (12), 2000314. https://doi.org/https://doi.org/10.1002/pssb.202000314.
(26) Botka, B.; Füstös, M. E.; Tóháti, H. M.; Németh, K.; Klupp, G.; Szekrényes, Z.; Kocsis, D.; Utczás, M.; Székely, E.; Váczi, T.; Tarczay, G.; Hackl, R.; Chamberlain, T. W.; Khlobystov, A. N.; Kamarás, K. Interactions and Chemical Transformations of Coronene Inside and Outside Carbon Nanotubes. *Small* **2014**, *10* (7), 1369–1378. https://doi.org/https://doi.org/10.1002/smll.201302613.
(27) Botka, B.; Füstös, M. E.; Klupp, G.; Kocsis, D.; Székely, E.; Utczás, M.; Simándi, B.; Botos, Á.; Hackl, R.; Kamarás, K. Low-Temperature Encapsulation of Coronene in Carbon Nanotubes. *Phys. status solidi* **2012**, *249* (12), 2432–2435. https://doi.org/https://doi.org/10.1002/pssb.201200349.
(28) Botos, Á.; Khlobystov, A. N.; Botka, B.; Hackl, R.; Székely, E.; Simándi, B.; Kamarás, K. Investigation of Fullerene Encapsulation in Carbon Nanotubes Using a Complex Approach Based on Vibrational Spectroscopy. *Phys. status solidi* **2010**, *247* (11–12), 2743–2745. https://doi.org/10.1002/pssb.201000375.
(29) Badon, A.; Marceau, J.-B.; Allard, C.; Fossard, F.; Loiseau, A.; Cognet, L.; Flahaut, E.; Recher, G.; Izard, N.; Martel, R.; Gaufrès, E. Fluorescence Anisotropy Using Highly Polarized Emitting Dyes Confined inside BNNTs. *Mater. Horizons* **2023**, *10* (3), 983–992. https://doi.org/10.1039/D2MH01239A.
(30) Zaumseil, J. Luminescent Defects in Single-Walled Carbon Nanotubes for

Applications. *Adv. Opt. Mater.* **2022**, *10* (2), 2101576. https://doi.org/10.1002/adom.202101576.
(31) He, X.; Htoon, H.; Doorn, S. K.; Pernice, W. H. P.; Pyatkov, F.; Krupke, R.; Jeantet, A.; Chassagneux, Y.; Voisin, C. Carbon Nanotubes as Emerging Quantum-Light Sources. *Nature Mater.* **2018**, *17* (8), 663–670. https://doi.org/10.1038/s41563-018-0109-2.
(32) Cambré, S.; Wenseleers, W.; Čulin, J.; Van Doorslaer, S.; Fonseca, A.; Nagy, J. B.; Goovaerts, E. Characterisation of Nanohybrids of Porphyrins with Metallic and Semiconducting Carbon Nanotubes by EPR and Optical Spectroscopy. *ChemPhysChem* **2008**, *9* (13), 1930–1941. https://doi.org/10.1002/cphc.200800317.
(33) Setaro, A.; Bluemmel, P.; Maity, C.; Hecht, S.; Reich, S. Non-Covalent Functionalization of Individual Nanotubes with Spiropyran-Based Molecular Switches. *Adv. Funct. Mater.* **2012**, *22* (11), 2425–2431. https://doi.org/10.1002/adfm.201102451.
(34) Wang, R. K.; Chen, W.-C.; Campos, D. K.; Ziegler, K. J. Swelling the Micelle Core Surrounding Single-Walled Carbon Nanotubes with Water-Immiscible Organic Solvents. *J. Am. Chem. Soc.* **2008**, *130* (48), 16330–16337. https://doi.org/10.1021/ja806586v.
(35) Delport, G.; Orcin-Chaix, L.; Campidelli, S.; Voisin, C.; Lauret, J. S. Controlling the Kinetics of the Non-Covalent Functionalization of Carbon Nanotubes Using Sub-Cmc Dilutions in a Co-Surfactant Environment. *Nanoscale* **2017**. https://doi.org/10.1039/c6nr08942a.
(36) Roquelet, C.; Lauret, J.-S.; Alain-Rizzo, V.; Voisin, C.; Fleurier, R.; Delarue, M.; Garrot, D.; Loiseau, A.; Roussignol, P.; Delaire, J. A.; Deleporte, E. Π-Stacking Functionalization of Carbon Nanotubes through Micelle Swelling. *ChemPhysChem* **2010**, *11* (8), 1667–1672. https://doi.org/10.1002/cphc.201000067.
(37) Clavé, G.; Delport, G.; Roquelet, C.; Lauret, J.-S.; Deleporte, E.; Vialla, F.; Langlois, B.; Parret, R.; Voisin, C.; Roussignol, P.; Jousselme, B.; Gloter, A.; Stephan, O.; Filoramo, A.; Derycke, V.; Campidelli, S. Functionalization of Carbon Nanotubes through Polymerization in Micelles: A Bridge between the Covalent and Noncovalent Methods. *Chem. Mater.* **2013**, *25* (13), 2700–2707. https://doi.org/10.1021/cm401312v.
(38) Glaeske, M.; Bluemmel, P.; Juergensen, S.; Setaro, A.; Reich, S. Dipole-Switch Induced Modification of the Emissive Response of Carbon Nanotubes. *J. Phys. Condens. Matter* **2017**. https://doi.org/10.1088/1361-648X/aa8dcf.
(39) Setaro, A.; Adeli, M.; Glaeske, M.; Przyrembel, D.; Bisswanger, T.; Gordeev, G.; Maschietto, F.; Faghani, A.; Paulus, B.; Weinelt, M.; Arenal, R.; Haag, R.; Reich, S. Preserving π-Conjugation in Covalently Functionalized Carbon Nanotubes for Optoelectronic Applications. *Nature Commun.* **2017**, *8* (1), 14281. https://doi.org/10.1038/ncomms14281.
(40) Godin, A. G.; Setaro, A.; Gandil, M.; Haag, R.; Adeli, M.; Reich, S.; Cognet, L. Photoswitchable Single-Walled Carbon Nanotubes for Super-Resolution Microscopy in the near-Infrared. *Sci. Adv.* **2019**, *5* (9), eaax1166. https://doi.org/10.1126/sciadv.aax1166.
(41) Graf, A.; Zakharko, Y.; Schießl, S. P.; Backes, C.; Pfohl, M.; Flavel, B. S.; Zaumseil, J. Large Scale, Selective Dispersion of Long Single-Walled Carbon Nanotubes with High Photoluminescence Quantum Yield by Shear Force Mixing. *Carbon* **2016**, *105*, 593–599. https://doi.org/10.1016/j.carbon.2016.05.002.
(42) Cambré, S.; Wenseleers, W. Separation and Diameter-Sorting of Empty (End-Capped) and Water-Filled (Open) Carbon Nanotubes by Density Gradient Ultracentrifugation.

Angew. Chemie Int. Ed. **2011**, *50* (12), 2764–2768. https://doi.org/10.1002/anie.201007324.
(43) Fagan, J. A.; Huh, J. Y.; Simpson, J. R.; Blackburn, J. L.; Holt, J. M.; Larsen, B. A.; Walker, A. R. H. Separation of Empty and Water-Filled Single-Wall Carbon Nanotubes. *ACS Nano* **2011**, *5* (5), 3943–3953. https://doi.org/10.1021/nn200458t.
(44) Gaufrès, E.; Tang, N. Y. W.; Lapointe, F.; Cabana, J.; Nadon, M.-A.; Cottenye, N.; Raymond, F.; Szkopek, T.; Martel, R. Giant Raman Scattering from J-Aggregated Dyes inside Carbon Nanotubes for Multispectral Imaging. *Nature Photon.* **2014**, *8* (1), 72–78. https://doi.org/10.1038/nphoton.2013.309.
(45) Yanagi, K.; Iakoubovskii, K.; Kazaoui, S.; Minami, N.; Maniwa, Y.; Miyata, Y.; Kataura, H. Light-Harvesting Function of β -Carotene inside Carbon Nanotubes. *Phys. Rev. B - Condens. Matter Mater. Phys.* **2006**. https://doi.org/10.1103/PhysRevB.74.155420.
(46) Cambré, S.; Wenseleers, W.; Goovaerts, E. Endohedral Copper(II)Acetylacetonate/Single-Walled Carbon Nanotube Hybrids Characterized by Electron Paramagnetic Resonance. *J. Phys. Chem. C* **2009**, *113* (31), 13505–13514. https://doi.org/10.1021/jp903724h.
(47) Hermosilla-Palacios, M. A.; Martinez, M.; Doud, E. A.; Hertel, T.; Spokoyny, A. M.; Cambré, S.; Wenseleers, W.; Kim, Y.-H.; Ferguson, A. J.; Blackburn, J. L. Carrier Density and Delocalization Signatures in Doped Carbon Nanotubes from Quantitative Magnetic Resonance. *Nanoscale Horizons* **2024**, *9* (2), 278–284. https://doi.org/10.1039/D3NH00480E.
(48) Yanagi, K.; Moriya, R.; Cuong, N. T.; Otani, M.; Okada, S. Charge Manipulation in Molecules Encapsulated Inside Single-Wall Carbon Nanotubes. *Phys. Rev. Lett.* **2013**, *110* (8), 086801. https://doi.org/10.1103/PhysRevLett.110.086801.
(49) Vialla, F.; Roquelet, C.; Langlois, B.; Delport, G.; Santos, S. M.; Deleporte, E.; Roussignol, P.; Delalande, C.; Voisin, C.; Lauret, J.-S. Chirality Dependence of the Absorption Cross Section of Carbon Nanotubes. *Phys. Rev. Lett.* **2013**, *111* (13), 137402. https://doi.org/10.1103/PhysRevLett.111.137402.
(50) Bachilo, S. M.; Strano, M. S.; Kittrell, C.; Hauge, R. H.; Smalley, R. E.; Weisman, R. B. Structure-Assigned Optical Spectra of Single-Walled Carbon Nanotubes. *Science* **2002**, *298* (5602), 2361 LP – 2366. https://doi.org/10.1126/science.1078727.
(51) Roquelet, C.; Garrot, D.; Lauret, J. S.; Voisin, C.; Alain-Rizzo, V.; Roussignol, P.; Delaire, J. A.; Deleporte, E. Quantum Efficiency of Energy Transfer in Noncovalent Carbon Nanotube/Porphyrin Compounds. *Appl. Phys. Lett.* **2010**, *97* (14). https://doi.org/10.1063/1.3496470.
(52) Chiashi, S.; Saito, Y.; Kato, T.; Konabe, S.; Okada, S.; Yamamoto, T.; Homma, Y. Confinement Effect of Sub-Nanometer Difference on Melting Point of Ice-Nanotubes Measured by Photoluminescence Spectroscopy. *ACS Nano* **2019**, *3* (13), 1177–1182. https://doi.org/10.1021/acsnano.8b06041.
(53) Ma, X.; Cambré, S.; Wenseleers, W.; Doorn, S. K.; Htoon, H. Quasiphase Transition in a Single File of Water Molecules Encapsulated in (6,5) Carbon Nanotubes Observed by Temperature-Dependent Photoluminescence Spectroscopy. *Phys. Rev. Lett.* **2017**, *118* (2), 027402. https://doi.org/10.1103/PhysRevLett.118.027402.
(54) Nishihara, T.; Okano, M.; Yamada, Y.; Kanemitsu, Y. Review—Photophysics of Trions in Single-Walled Carbon Nanotubes. *ECS J. Solid State Sci. Technol.* **2017**, *6* (6), M3062–M3064. https://doi.org/10.1149/2.0091706jss.
(55) Kwon, H.; Kim, M.; Nutz, M.; Hartmann, N. F.; Perrin, V.; Meany, B.; Hofmann, M. S.; Clark, C. W.; Htoon, H.; Doorn, S. K.; Högele, A.; Wang, Y. Probing Trions at Chemically Tailored Trapping Defects. *ACS Cent. Sci.* **2019**, *5* (11), 1786–1794.

https://doi.org/10.1021/acscentsci.9b00707.
(56) He, X.; Hartmann, N. F.; Ma, X.; Kim, Y.; Ihly, R.; Blackburn, J. L.; Gao, W.; Kono, J.; Yomogida, Y.; Hirano, A.; Tanaka, T.; Kataura, H.; Htoon, H.; Doorn, S. K. Tunable Room-Temperature Single-Photon Emission at Telecom Wavelengths from Sp3 Defects in Carbon Nanotubes. *Nature Photon.* **2017**, *11* (9), 577–582. https://doi.org/10.1038/nphoton.2017.119.
(57) Brozena, A. H.; Kim, M.; Powell, L. R.; Wang, Y. Controlling the Optical Properties of Carbon Nanotubes with Organic Colour-Centre Quantum Defects. *Nat. Rev. Chem.* **2019**, *3* (6), 375–392. https://doi.org/10.1038/s41570-019-0103-5.
(58) Garrot, D.; Langlois, B.; Roquelet, C.; Michel, T.; Roussignol, P.; Delalande, C.; Deleporte, E.; Lauret, J. S.; Voisin, C. Time-Resolved Investigation of Excitation Energy Transfer in Carbon Nanotube-Porphyrin Compounds. *J. Phys. Chem. C* **2011**. https://doi.org/10.1021/jp207267e.
(59) Piao, Y.; Meany, B.; Powell, L. R.; Valley, N.; Kwon, H.; Schatz, G. C.; Wang, Y. Brightening of Carbon Nanotube Photoluminescence through the Incorporation of Sp3 Defects. *Nature. Chem.* **2013**, *5* (10), 840–845. https://doi.org/10.1038/nchem.1711.
(60) Sebastian, F. L.; Zorn, N. F.; Settele, S.; Lindenthal, S.; Berger, F. J.; Bendel, C.; Li, H.; Flavel, B. S.; Zaumseil, J. Absolute Quantification of Sp 3 Defects in Semiconducting Single-Wall Carbon Nanotubes by Raman Spectroscopy. *J. Phys. Chem. Lett.* **2022**, *13* (16), 3542–3548. https://doi.org/10.1021/acs.jpclett.2c00758.
(61) Gaufrès, E.; Tang, N. Y. W.; Lapointe, F.; Cabana, J.; Nadon, M. A.; Cottenye, N.; Raymond, F.; Szkopek, T.; Martel, R. Giant Raman Scattering from J-Aggregated Dyes inside Carbon Nanotubes for Multispectral Imaging. *Nature Photon.* **2014**. https://doi.org/10.1038/nphoton.2013.309.
(62) Araujo, P. T.; Doorn, S. K.; Kilina, S.; Tretiak, S.; Einarsson, E.; Maruyama, S.; Chacham, H.; Pimenta, M. A.; Jorio, A. Third and Fourth Optical Transitions in Semiconducting Carbon Nanotubes. *Phys. Rev. Lett.* **2007**, *98* (6), 067401. https://doi.org/10.1103/PhysRevLett.98.067401.
(63) O'Connell, M. J.; Sivaram, S.; Doorn, S. K. Near-Infrared Resonance Raman Excitation Profile Studies of Single-Walled Carbon Nanotube Intertube Interactions: A Direct Comparison of Bundled and Individually Dispersed <math Display="inline"> <mrow> <mi Mathvariant="normal">HiPco</Mi> </Mrow> </Math>. *Phys. Rev. B* **2004**, *69* (23), 235415. https://doi.org/10.1103/PhysRevB.69.235415.
(64) Finnie, P.; Ouyang, J.; Fagan, J. A. Broadband Full-Spectrum Raman Excitation Mapping Reveals Intricate Optoelectronic–Vibrational Resonance Structure of Chirality-Pure Single-Walled Carbon Nanotubes. *ACS Nano* **2023**, *17* (8), 7285–7295. https://doi.org/10.1021/acsnano.2c10524.
(65) Jorio, A.; Saito, R. Raman Spectroscopy for Carbon Nanotube Applications. *J. Appl. Phys.* **2021**, *129* (2). https://doi.org/10.1063/5.0030809.
(66) Heeg, S.; Shi, L.; Poulikakos, L. V; Pichler, T.; Novotny, L. Carbon Nanotube Chirality Determines Properties of Encapsulated Linear Carbon Chain. *Nano Lett.* **2018**, *18* (9), 5426–5431. https://doi.org/10.1021/acs.nanolett.8b01681.
(67) Shi, L.; Rohringer, P.; Wanko, M.; Rubio, A.; Waßerroth, S.; Reich, S.; Cambré, S.; Wenseleers, W.; Ayala, P.; Pichler, T. Electronic Band Gaps of Confined Linear Carbon Chains Ranging from Polyyne to Carbyne. *Phys. Rev. Mater.* **2017**, *1* (7). https://doi.org/10.1103/PhysRevMaterials.1.075601.
(68) Martinati, M.; Wenseleers, W.; Shi, L.; Pratik, S. M.; Rohringer, P.; Cui, W.; Pichler, T.; Coropceanu, V.; Brédas, J.-L.; Cambré, S. Electronic Structure of Confined Carbyne from Joint Wavelength-Dependent Resonant Raman Spectroscopy and Density Functional Theory Investigations. *Carbon* **2022**, *189*, 276–283.

https://doi.org/https://doi.org/10.1016/j.carbon.2021.12.059.
(69) Heeg, S.; Shi, L.; Pichler, T.; Novotny, L. Raman Resonance Profile of an Individual Confined Long Linear Carbon Chain. *Carbon* **2018**, *139*, 581–585. https://doi.org/https://doi.org/10.1016/j.carbon.2018.07.007.
(70) Kuzmany, H.; Shi, L.; Martinati, M.; Cambré, S.; Wenseleers, W.; Kürti, J.; Koltai, J.; Kukucska, G.; Cao, K.; Kaiser, U.; Saito, T.; Pichler, T. Well-Defined Sub-Nanometer Graphene Ribbons Synthesized inside Carbon Nanotubes. *Carbon* **2021**, *171*, 221–229. https://doi.org/10.1016/j.carbon.2020.08.065.
(71) Shi, L.; Rohringer, P.; Wanko, M.; Rubio, A.; Waßerroth, S.; Reich, S.; Cambré, S.; Wenseleers, W.; Ayala, P.; Pichler, T. Electronic Band Gaps of Confined Linear Carbon Chains Ranging from Polyyne to Carbyne. *Phys. Rev. Mater.* **2017**, *1* (7), 075601. https://doi.org/10.1103/PhysRevMaterials.1.075601.
(72) Shi, L.; Rohringer, P.; Suenaga, K.; Niimi, Y.; Kotakoski, J.; Meyer, J. C.; Peterlik, H.; Wanko, M.; Cahangirov, S.; Rubio, A.; Lapin, Z. J.; Novotny, L.; Ayala, P.; Pichler, T. Confined Linear Carbon Chains as a Route to Bulk Carbyne. *Nature Mater.* **2016**, *15* (6), 634–639. https://doi.org/10.1038/nmat4617.
(73) Tschannen, C. D.; Gordeev, G.; Reich, S.; Shi, L.; Pichler, T.; Frimmer, M.; Novotny, L.; Heeg, S. Raman Scattering Cross Section of Confined Carbyne. *Nano Lett.* **2020**, *20* (9), 6750–6755. https://doi.org/10.1021/acs.nanolett.0c02632.
(74) Wasserroth, S.; Heeg, S.; Mueller, N. S.; Kusch, P.; Hübner, U.; Gaufrès, E.; Tang, N. Y.-W.; Martel, R.; Vijayaraghavan, A.; Reich, S. Resonant, Plasmonic Raman Enhancement of α-6T Molecules Encapsulated in Carbon Nanotubes. *J. Phys. Chem. C* **2019**, *123* (16), 10578–10585. https://doi.org/10.1021/acs.jpcc.9b01600.
(75) Delport, G.; Vialla, F.; Roquelet, C.; Campidelli, S.; Voisin, C.; Lauret, J. S. Davydov Splitting and Self-Organization in a Porphyrin Layer Noncovalently Attached to Single Wall Carbon Nanotubes. *Nano Lett.* **2017**. https://doi.org/10.1021/acs.nanolett.7b02996.
(76) Kim, M.; Chen, C.; Wang, P.; Mulvey, J. J.; Yang, Y.; Wun, C.; Antman-Passig, M.; Luo, H.-B.; Cho, S.; Long-Roche, K.; Ramanathan, L. V; Jagota, A.; Zheng, M.; Wang, Y.; Heller, D. A. Detection of Ovarian Cancer via the Spectral Fingerprinting of Quantum-Defect-Modified Carbon Nanotubes in Serum by Machine Learning. *Nat. Biomed. Eng.* **2022**, *6* (3), 267–275. https://doi.org/10.1038/s41551-022-00860-y.
(77) Ackermann, J.; Metternich, J. T.; Herbertz, S.; Kruss, S. Biosensing with Fluorescent Carbon Nanotubes. *Angew. Chemie Int. Ed.* **2022**, *61* (18), e202112372. https://doi.org/https://doi.org/10.1002/anie.202112372.
(78) Ackermann, J.; Stegemann, J.; Smola, T.; Reger, E.; Jung, S.; Schmitz, A.; Herbertz, S.; Erpenbeck, L.; Seidl, K.; Kruss, S. High Sensitivity Near-Infrared Imaging of Fluorescent Nanosensors. *Small* **2023**, *n/a* (n/a), 2206856. https://doi.org/https://doi.org/10.1002/smll.202206856.
(79) Kagan, B.; Hendler-Neumark, A.; Wulf, V.; Kamber, D.; Ehrlich, R.; Bisker, G. Super-Resolution Near-Infrared Fluorescence Microscopy of Single-Walled Carbon Nanotubes Using Deep Learning. *Adv. Photonics Res.* **2022**, *3* (11), 2200244. https://doi.org/https://doi.org/10.1002/adpr.202200244.
(80) Sharaga, E.; Hendler-Neumark, A.; Kamber, D.; Bisker, G. Spatiotemporal Tracking of Near-Infrared Fluorescent Single-Walled Carbon Nanotubes in C. Elegans Nematodes Confined in a Microfluidics Platform (Adv. Mater. Technol. 5/2024). *Adv. Mater. Technol.* **2024**, *9* (5). https://doi.org/10.1002/admt.202470021.
(81) Berger, F. J.; de Sousa, J. A.; Zhao, S.; Zorn, N. F.; El Yumin, A. A.; Quintana García, A.; Settele, S.; Högele, A.; Crivillers, N.; Zaumseil, J. Interaction of Luminescent Defects in Carbon Nanotubes with Covalently Attached Stable Organic Radicals. *ACS*

Nano **2021**, *15* (3), 5147–5157. https://doi.org/10.1021/acsnano.0c10341.
(82) Lin, C.-W.; Bachilo, S. M.; Weisman, R. B. Delayed Fluorescence from Carbon Nanotubes through Singlet Oxygen-Sensitized Triplet Excitons. *J. Am. Chem. Soc.* **2020**, *142* (50), 21189–21196. https://doi.org/10.1021/jacs.0c10557.
(83) Arellano, L. M.; Gobeze, H. B.; Gómez-Escalonilla, M. J.; Fierro, J. L. G.; D'Souza, F.; Langa, F. Triplet Photosensitizer-Nanotube Conjugates: Synthesis, Characterization and Photochemistry of Charge Stabilizing, Palladium Porphyrin/Carbon Nanotube Conjugates. *Nanoscale* **2020**, *12* (17), 9890–9898. https://doi.org/10.1039/D0NR02136A.
(84) Sandanayaka, A. S. D.; Subbaiyan, N. K.; Das, S. K.; Chitta, R.; Maligaspe, E.; Hasobe, T.; Ito, O.; D'Souza, F. Diameter-Sorted SWCNT–Porphyrin and SWCNT–Phthalocyanine Conjugates for Light-Energy Harvesting. *ChemPhysChem* **2011**, *12* (12), 2266–2273. https://doi.org/10.1002/cphc.201100377.
(85) Gao, J.; Blondeau, P.; Salice, P.; Menna, E.; Bártová, B.; Hébert, C.; Leschner, J.; Kaiser, U.; Milko, M.; Ambrosch-Draxl, C.; Loi, M. A. Electronic Interactions between "Pea" and "Pod": The Case of Oligothiophenes Encapsulated in Carbon Nanotubes. *Small* **2011**, *7* (13), 1807–1815. https://doi.org/10.1002/smll.201100319.
(86) Cambré, S.; Wenseleers, W.; Goovaerts, E.; Resasco, D. E. Determination of the Metallic/Semiconducting Ratio in Bulk Single-Wall Carbon Nanotube Samples by Cobalt Porphyrin Probe Electron Paramagnetic Resonance Spectroscopy. *ACS Nano* **2010**, *4* (11), 6717–6724. https://doi.org/10.1021/nn102222w.
(87) Roquelet, C.; Garrot, D.; Lauret, J. S.; Voisin, C.; Alain-Rizzo, V.; Roussignol, P.; Delaire, J. A.; Deleporte, E. Quantum Efficiency of Energy Transfer in Noncovalent Carbon Nanotube/Porphyrin Compounds. *Appl. Phys. Lett.* **2010**, *97* (14), 141918. https://doi.org/10.1063/1.3496470.
(88) Iijima, S. Helical Microtubules of Graphitic Carbon. *Nature* **1991**, *354* (6348), 56–58. https://doi.org/10.1038/354056a0.
(89) Loiseau, A.; Willaime, F.; Demoncy, N.; Hug, G.; Pascard, H. Boron Nitride Nanotubes with Reduced Numbers of Layers Synthesized by Arc Discharge. *Phys. Rev. Lett.* **1996**, *76* (25), 4737–4740. https://doi.org/10.1103/PhysRevLett.76.4737.
(90) Loi, M. A.; Gao, J.; Cordella, F.; Blondeau, P.; Menna, E.; Bártová, B.; Hébert, C.; Lazar, S.; Botton, G. A.; Milko, M.; Ambrosch-Draxl, C. Encapsulation of Conjugated Oligomers in Single-Walled Carbon Nanotubes: Towards Nanohybrids for Photonic Devices. *Adv. Mater.* **2010**. https://doi.org/10.1002/adma.200903527.
(91) Krivanek, O. L.; Chisholm, M. F.; Nicolosi, V.; Pennycook, T. J.; Corbin, G. J.; Dellby, N.; Murfitt, M. F.; Own, C. S.; Szilagyi, Z. S.; Oxley, M. P.; Pantelides, S. T.; Pennycook, S. J. Atom-by-Atom Structural and Chemical Analysis by Annular Dark-Field Electron Microscopy. *Nature* **2010**, *464* (7288), 571–574. https://doi.org/10.1038/nature08879.
(92) Jin, C.; Lin, F.; Suenaga, K.; Iijima, S. Fabrication of a Freestanding Boron Nitride Single Layer and Its Defect Assignments. *Phys. Rev. Lett.* **2009**, *102* (19), 195505. https://doi.org/10.1103/PhysRevLett.102.195505.
(93) Pan, C. T.; Nair, R. R.; Bangert, U.; Ramasse, Q.; Jalil, R.; Zan, R.; Seabourne, C. R.; Scott, A. J. Nanoscale Electron Diffraction and Plasmon Spectroscopy of Single- and Few-Layer Boron Nitride. *Phys. Rev. B* **2012**, *85* (4), 045440. https://doi.org/10.1103/PhysRevB.85.045440.
(94) Jiang, Y.; Chen, Z.; Han, Y.; Deb, P.; Gao, H.; Xie, S.; Purohit, P.; Tate, M. W.; Park, J.; Gruner, S. M.; Elser, V.; Muller, D. A. Electron Ptychography of 2D Materials to Deep Sub-Ångström Resolution. *Nature* **2018**, *559* (7714), 343–349. https://doi.org/10.1038/s41586-018-0298-5.

(95) Kaiser, U.; Biskupek, J.; Meyer, J. C.; Leschner, J.; Lechner, L.; Rose, H.; Stöger-Pollach, M.; Khlobystov, A. N.; Hartel, P.; Müller, H.; Haider, M.; Eyhusen, S.; Benner, G. Transmission Electron Microscopy at 20kV for Imaging and Spectroscopy. *Ultramicroscopy* **2011**, *111* (8), 1239–1246. https://doi.org/10.1016/j.ultramic.2011.03.012.
(96) Almadori, Y.; Alvarez, L.; Le Parc, R.; Aznar, R.; Fossard, F.; Loiseau, A.; Jousselme, B.; Campidelli, S.; Hermet, P.; Belhboub, A.; Rahmani, A.; Saito, T.; Bantignies, J.-L. Chromophore Ordering by Confinement into Carbon Nanotubes. *J. Phys. Chem. C* **2014**, *118* (33), 19462–19468. https://doi.org/10.1021/jp505804d.
(97) Badon, A.; Marceau, J.-B.; Allard, C.; Fossard, F.; Loiseau, A.; Cognet, L.; Flahaut, E.; Recher, G.; Izard, N.; Martel, R.; Gaufrès, E. Fluorescence Anisotropy Using Highly Polarized Emitting Dyes Confined inside BNNTs. *Mater. Horizons* **2023**, *10* (3), 983–992. https://doi.org/10.1039/D2MH01239A.
(98) Arenal, R.; Stéphan, O.; Kociak, M.; Taverna, D.; Loiseau, A.; Colliex, C. Electron Energy Loss Spectroscopy Measurement of the Optical Gaps on Individual Boron Nitride Single-Walled and Multiwalled Nanotubes. *Phys. Rev. Lett.* **2005**, *95* (12), 127601. https://doi.org/10.1103/PhysRevLett.95.127601.
(99) Ramasse, Q. M.; Seabourne, C. R.; Kepaptsoglou, D.-M.; Zan, R.; Bangert, U.; Scott, A. J. Probing the Bonding and Electronic Structure of Single Atom Dopants in Graphene with Electron Energy Loss Spectroscopy. *Nano Lett.* **2013**, *13* (10), 4989–4995. https://doi.org/10.1021/nl304187e.
(100) Kinyanjui, M. K.; Kramberger, C.; Pichler, T.; Meyer, J. C.; Wachsmuth, P.; Benner, G.; Kaiser, U. Direct Probe of Linearly Dispersing 2D Interband Plasmons in a Free-Standing Graphene Monolayer. *EPL (Europhysics Lett.* **2012**, *97* (5), 57005. https://doi.org/10.1209/0295-5075/97/57005.
(101) Fossard, F.; Sponza, L.; Schué, L.; Attaccalite, C.; Ducastelle, F.; Barjon, J.; Loiseau, A. Angle-Resolved Electron Energy Loss Spectroscopy in Hexagonal Boron Nitride. *Phys. Rev. B* **2017**, *96* (11), 115304. https://doi.org/10.1103/PhysRevB.96.115304.
(102) Gaufrès, E.; Fossard, F.; Gosselin, V.; Sponza, L.; Ducastelle, F.; Li, Z.; Louie, S. G.; Martel, R.; Côté, M.; Loiseau, A. Momentum-Resolved Dielectric Response of Free-Standing Mono-, Bi-, and Trilayer Black Phosphorus. *Nano Lett.* **2019**, *19* (11), 8303–8310. https://doi.org/10.1021/acs.nanolett.9b03928.
(103) Senga, R.; Suenaga, K.; Barone, P.; Morishita, S.; Mauri, F.; Pichler, T. Position and Momentum Mapping of Vibrations in Graphene Nanostructures. *Nature* **2019**, *573* (7773), 247–250. https://doi.org/10.1038/s41586-019-1477-8.
(104) Kociak, M.; Blazit, J.-D.; Bocher, L.; Brun, N.; Colliex, C.; de Frutos, M.; Gloter, A.; Li, X.; Tencé, M.; Tizei, L. H. G.; Walls, M.; Zobelli, A.; Stéphan, O. New Directions Toward Nanophysics Experiments in STEM. *Microsc. Microanal.* **2018**, *24* (S1), 434–435. https://doi.org/10.1017/S1431927618002660.
(105) Müller, K.; Krause, F. F.; Béché, A.; Schowalter, M.; Galioit, V.; Löffler, S.; Verbeeck, J.; Zweck, J.; Schattschneider, P.; Rosenauer, A. Atomic Electric Fields Revealed by a Quantum Mechanical Approach to Electron Picodiffraction. *Nature Commun.* **2014**, *5* (1), 5653. https://doi.org/10.1038/ncomms6653.
(106) da Silva, B. C.; Sadre Momtaz, Z.; Monroy, E.; Okuno, H.; Rouviere, J.-L.; Cooper, D.; Den Hertog, M. I. Assessment of Active Dopants and p–n Junction Abruptness Using In Situ Biased 4D-STEM. *Nano Lett.* **2022**, *22* (23), 9544–9550. https://doi.org/10.1021/acs.nanolett.2c03684.
(107) Haas, B.; Rouvière, J.-L.; Boureau, V.; Berthier, R.; Cooper, D. Direct Comparison of Off-Axis Holography and Differential Phase Contrast for the Mapping of Electric Fields in Semiconductors by Transmission Electron Microscopy. *Ultramicroscopy*

2019, *198*, 58–72. https://doi.org/10.1016/j.ultramic.2018.12.003.
(108) Beyer, A.; Munde, M. S.; Firoozabadi, S.; Heimes, D.; Grieb, T.; Rosenauer, A.; Müller-Caspary, K.; Volz, K. Quantitative Characterization of Nanometer-Scale Electric Fields via Momentum-Resolved STEM. *Nano Lett.* **2021**, *21* (5), 2018–2025. https://doi.org/10.1021/acs.nanolett.0c04544.
(109) Susana, L.; Gloter, A.; Tencé, M.; Zobelli, A. Direct Quantifying Charge Transfer by 4D-STEM: A Study on Perfect and Defective Hexagonal Boron Nitride. *ACS Nano* **2024**, *18* (10), 7424–7432. https://doi.org/10.1021/acsnano.3c10299.
(110) Corzilius, B.; Gembus, A.; Weiden, N.; Dinse, K. -P.; Hata, K. EPR Characterization of Catalyst-free SWNT and N@C 60 -based Peapods. *Phys. status solidi* **2006**, *243* (13), 3273–3276. https://doi.org/10.1002/pssb.200669115.
(111) Corzilius, B.; Dinse, K. P.; Hata, K. Single-Wall Carbon Nanotubes and Peapods Investigated by EPR. *Physical Chemistry Chemical Physics*. 2007. https://doi.org/10.1039/b707936m.
(112) Jakes, P.; Gembus, A.; Dinse, K.-P.; Hata, K. Electron Paramagnetic Resonance Investigation of Metalloendofullerene Derived Carbon Nanotube Peapods. *J. Chem. Phys.* **2008**, *128* (5). https://doi.org/10.1063/1.2825592.
(113) Qu, H.; Rayabharam, A.; Wu, X.; Wang, P.; Li, Y.; Fagan, J.; Aluru, N. R.; Wang, Y. Selective Filling of N-Hexane in a Tight Nanopore. *Nature Commun.* **2021**, *12* (1), 310. https://doi.org/10.1038/s41467-020-20587-1.
(114) Cambré, S.; Muyshondt, P.; Federicci, R.; Wenseleers, W. Chirality-Dependent Densities of Carbon Nanotubes by in Situ 2D Fluorescence-Excitation and Raman Characterisation in a Density Gradient after Ultracentrifugation. *Nanoscale* **2015**, *7* (47), 20015–20024. https://doi.org/10.1039/c5nr06020f.